Available online at www.sciencedirect.com
ScienceDirect
Journal of Hazardous Materials 150 (2008) 774–782
Journal of Hazardous Materials
www.elsevier.com/locate/jhazmat

Adsorption of malachite green from aqueous solution onto carbon prepared from Arundo donax root

Jian Zhang *, Yan Li, Chenglu Zhang, Yuming Jing

School of Environmental Science and Engineering, Shandong University, Jinan 250100, China

Received 10 December 2006; received in revised form 9 May 2007; accepted 9 May 2007
Available online 16 May 2007

Abstract

Arundo donax root carbon (ADRC), a new adsorbent, was prepared from Arundo donax root by carbonization. The surface area of the adsorbent was determined 158 m^2/g by N_2 adsorption isotherm. Batch adsorption experiments were carried out for the removal of malachite green (MG) from aqueous solution using ADRC as adsorbent. The effects of various parameters such as solution pH (3–10), carbon dose (0.15–1.0 g/100 ml) and initial MG concentration (10–100 mg/l) on the adsorption system were investigated. The effective pH was 5–7 and the optimum adsorbent dose was found to be 0.6 g/100 ml. Equilibrium experimental data at 293, 303 and 313 K were better represented by Langmuir isotherm than Freundlich isotherm using linear and non-linear methods. Thermodynamic parameters such as ΔG, ΔH and ΔS were also calculated. The negative Gibbs free energy change and the positive enthalpy change indicated the spontaneous and endothermic nature of the adsorption. The adsorption equilibrium time was 180 min. Adsorption kinetics was determined using pseudo-first-order model, pseudo-second-order model and intraparticle diffusion model. The results showed that the adsorption of MG onto ADRC followed pseudo-second-order model.

Keywords: Arundo donax root carbon; Malachite green; Adsorption; Isotherm; Kinetics

1. Introduction

As a basic and cationic dye, malachite green (MG) has been widely used for the dyeing of leather, wool and silk as well as in distilleries [1,2]. In addition, MG also is used as a fungicide and antiseptic in aquaculture industry to control fish parasites and disease. But recently, the compound, a triphenylmethane dye, has been found exhibiting carcinogenic, genotoxic, mutagenic and teratogenic properties according to the reports about animal study [3] due to the presence of nitrogen [2]. The properties make it difficult to biodegrade MG or remove MG from aqueous solution [4,5]. Among the techniques for removal of dyes from wastewater, adsorption has been proved to be an effective and attractive process [6,7] because of its inexpensive nature and ease of operation [8]. Gupta et al. have contributed significantly on dye adsorptive removal for exploiture of many low-cost materials as adsorbents [9–15]. Low-cost adsorbents for the removal of various pollutants including dyes have been reviewed by Gupta and Ali [16]. In previous study, many adsorbents have been investigated for the removal of MG from its solution, including bottom ash [2], wheat bran [4], waste apricot [17,18], rice husk-based active carbon [19–21], formaldehyde-treated and sulphuric acid-treated sawdust [22,23], de-oiled soya [24], hen feathers [25], activated charcoal [26], bentonite clay [27], lignite [28], iron humate [29], bagasse fly ash [30], activated slag [31], sugar cane dust [5] and modified peat [32].

Arundo donax, a hydrophyte, is widely distributed in China. This plant has a developed tuberous root system and generally produces large and continuous root masses [33]. After the clump above soil is harvested for pulp in the paper industry, however, Arundo donax root is mostly discarded in Nansi Hu area of Shandong province in China. A survey of literature showed that no work has been done so far on utilization of Arundo donax root to prepare carbon as an adsorbent.

In the present study, Arundo donax root carbon (ADRC) prepared from Arundo donax root by carbonization was used as an adsorbent to remove MG from aqueous solution. The objective of our work was to examine the possibility of using ADRC to remove MG. Effects of different parameters including pH, adsorbent dose, initial dye concentration and contact time were

* Corresponding author. Tel.: +86 531 88361808; fax: +86 531 88364513.
E-mail address: zhangjian00@sdu.edu.cn (J. Zhang).

0304-3894/$ – see front matter © 2007 Published by Elsevier B.V.
doi:10.1016/j.jhazmat.2007.05.036

studied. The isotherms, kinetics and thermodynamics were also investigated.

2. Materials and methods

2.1. Preparation of ADRC

Arundo donax root used in this study was obtained from Nansi Hu area in Shandong province, washed with distilled water, dried and crushed. The Arundo donax root was carbonized at 300 °C under nitrogen atmosphere for 1 h in a tube furnace (SRJK-2-13, Beijing) and then cooled to room temperature. The carbonized product, ADRC, was washed with distilled water and then dried at 393 K for 3 h. The dried sample was grinded, sieved by standard sieves (Model Φ200) and stored in a desicator until required. The particle sizes of ADRC used in the study was 140–160 mesh.

The BET surface area was measured by N_2 adsorption isotherm at 77 K using QUADRASORB SI automated surface area and pore size analyzer (Quantachrome Corporation, USA). Brunauer–Emmett–Teller (BET) method and Barrett–Joyner–Halenda (BJH) method were used to calculate the surface area and the pore size distribution of ADRC, respectively. The zeta-potential of ADRC was measured by a zeta meter (JS94H, Shanghai) to indicate the charges at the surface of ADRC.

2.2. Dye solution

The dye, MG hydrochloride [C.I. = 42,000, chemical formula = $C_{23}H_{26}N_2Cl$, molecular weight 364.92; λ_{max} = 617 nm (reported)] was supplied by Laiyang Chemicals, Yantai, China. The molecular structure of MG is illustrated in Fig. 1. The stock solution (1000 mg/l) of MG was prepared by dissolving accurately weighed amount of the dye in distilled water. All working solutions of the desired concentration were obtained by diluting the stock solution with distilled water.

2.3. Batch adsorption equilibrium experiments

Batch adsorption experiments were conducted in order to evaluate the effects of solution pH, adsorbent dose and initial MG concentration. In each batch, the mixture of 100 ml dye solution of known pH, concentration and a known amount of ADRC was taken in 250 ml stoppered conical flask and mechanically agitated in a water bath shaker (SHZ-88) at a constant temperature. After reaching equilibrium, the mixture was filtered. The dye filtrate was then analyzed using a UV–vis spectrophotometer (UV-754, Shanghai) by measuring the absorbance at a wavelength corresponding to maximum absorbance, namely λ_{max} = 615 nm (experimentally obtained by us). The effect of solution pH on MG removal was investigated over a pH range of 3–10. The pH of solutions was measured by pH meter (Model pHS-3C). The pH was adjusted using 0.10 M HCl or 0.10 M NaOH aqueous solution. The experiments were also done by varying the amount of adsorbents (0.15–1.0 g/100 ml) and the concentration of dye solution (10–100 mg/l). For adsorption isotherm, dye solutions of different concentrations (30–100 mg/l) were shaken with the known amount of adsorbent (0.6 g) at 293, 303 and 313 K till the equilibrium was achieved. And then the residual MG concentration of the solution was determined. The amount of adsorbed MG per gram ADRC at equilibrium, q_e (mg/g), was obtained by

$$q_e = \frac{(C_0 - C_e)V}{W} \quad (1)$$

where C_0 and C_e (mg/l) are the concentrations of MG dye at initial and equilibrium, respectively. V (l) is the volume of the solution and W (g) is the weight of adsorbent used.

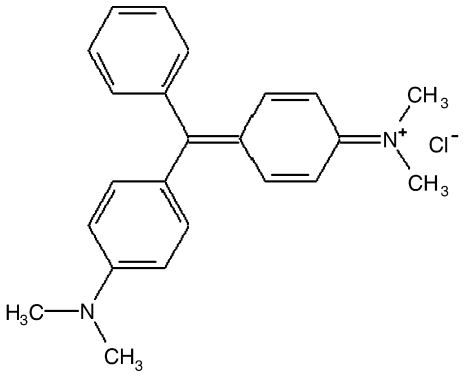

Fig. 1. Molecular structure of MG.

2.4. Adsorption kinetic studies

For the purpose of investigating the effect of contact time on the adsorption process and evaluating the kinetic properties, 12 g ADRC was added to 2000 ml dye solutions with the initial concentration of MG 30, 40 and 50 mg/l. The mixture was agitated on an electromagnetic stirrer (Model 78-1) at 30 ± 1 °C and 300 rpm. The stirring rate of 300 rpm was chosen in order to make ADRC homogenously to be dispersed in solution. At predetermined time intervals (0–210 min), 5 ml of samples was drawn and filtered. The filtrate samples were analyzed to determine the residual dye concentration. The adsorption amount at time t, q_t (mg/g), was calculated by the following equation:

$$q_t = \frac{(C_0 - C_t)V}{W} \quad (2)$$

where C_0 and C_t (mg/l) are the concentrations of MG dye at initial and any time t, respectively. V (l) is the solution volume and W (g) represents the mass of ADRC used.

3. Results and discussion

3.1. Characteristics of ADRC

The surface area of ADRC was found to be 158 m^2/g. Total pore volume is 0.041 cm^3/g and average pore diameter is 2.0 nm. ADRC has a relatively promising surface area although it was obtained from Arundo donax root only by carbonization process. Fig. 2 shows the pore size distribution of ADRC.

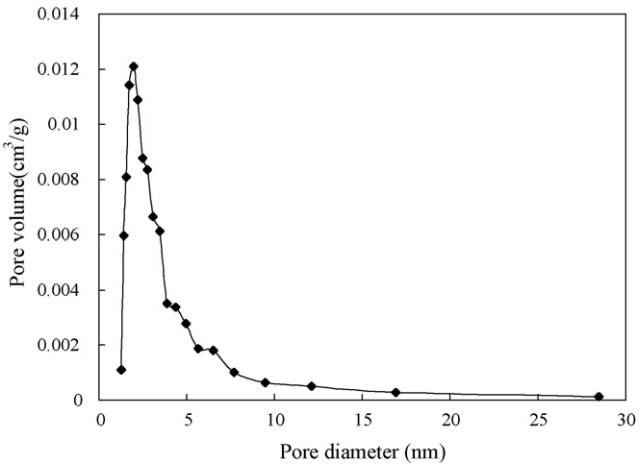

Fig. 2. Pore size distribution of ADRC.

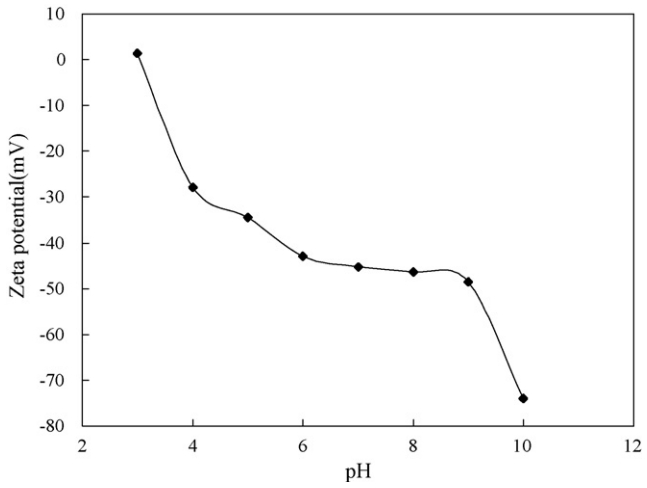

Fig. 4. The plot of the zeta-potential of ADRC vs. pH.

3.2. Effect of pH

Effect of solution pH on the adsorptive removal of MG by ADRC is shown in Fig. 3. As is known, pH can affect the structural stability of MG and therefore, its color intensity [30]. It was observed by naked eye during the adjustment of solution pH in the experiment that the dye color reduction began from pH 9. It may be due to the structural changes of MG molecules at higher pH. Hence, the dye removal increased sharply over a pH range of 8–10.

The color of MG was found to be stable over the pH range of 3.3–7. Dye removal by ADRC was minimum (28.4%) at pH 3.3, which increased to 41.8% at the pH of 7 (Fig. 3). Lower removal was due to the small adsorbent dosage (0.2 g/100 ml). The ADRC surface may contain large number of active sites and the MG uptake could be related to the active sites. Fig. 4 shows the plot of zeta-potential of ADRC versus pH. It was observed that ADRC exhibits negative zeta-potential values at the experimental conditions (i.e., pH > 3.3). As initial solution pH increased, the number of negatively charged active sites increased and positively charged sites decreased. Therefore, the electrostatic repulsion between the absorbent site and positively charged dye cations was lowed, which may result in the increase of the adsorption. Also, lower adsorptive removal of MG at acidic pH was due to the presence of excess hydrogen ion competing with MG cations for adsorption [23,30]. It may be seen from Fig. 3 that the dye removal was approximately no change in the pH range 5–7. Therefore, further experiments were performed at pH 5.0.

3.3. Effect of adsorbent dosage

The effect of adsorbent dosage on the adsorptive removal of MG by ADRC is shown in Fig. 5.

As can be seen, adsorption of MG increased with increasing the amount of ADRC and remained almost constant after increasing up to a certain limit. This can be attributed to increased adsorbent surface area and availability of more adsorption sites [23,30]. The optimum dosage was found to be 0.6 g/100 ml, as the dye removal was 86.4%.

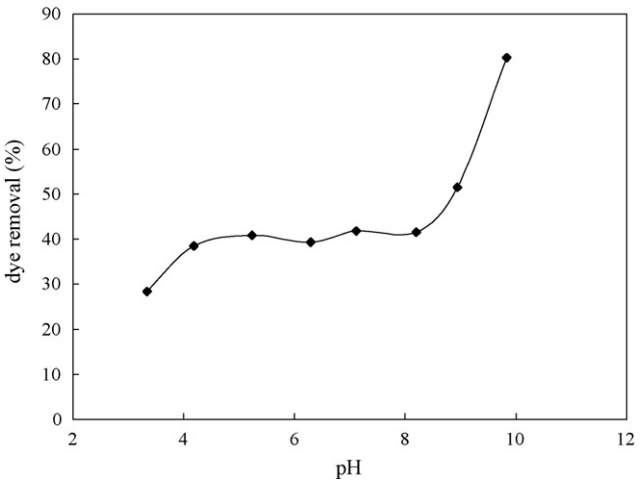

Fig. 3. Effect of solution pH on the adsorption of MG by ADRC (C_0 = 40 mg/l, ADRC dosage = 0.2 g/100 ml, temperature = 30 ± 1 °C, t = 180 min).

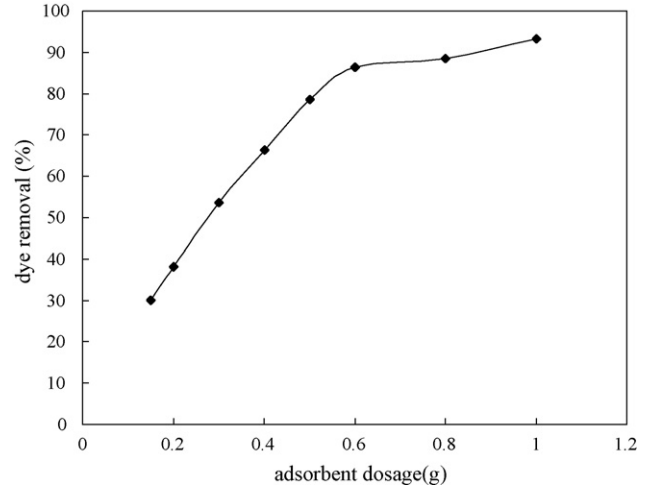

Fig. 5. Effect of adsorbent dosage on the adsorption of MG by ADRC (C_0 = 40 mg/l, pH 5, temperature = 30 ± 1 °C, t = 180 min).

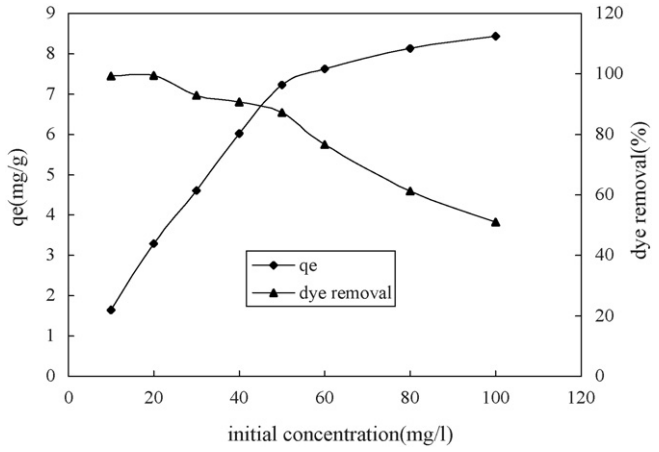

Fig. 6. Effect of initial dye concentration on the adsorption of MG by ADRC (ADRC dosage = 0.6 g/100 ml, pH 5, temperature = 30 ± 1 °C, t = 180 min).

Dye removal increased from 30.1 to 93.3% as the ADRC dose was increased from 0.15 to 1.0 g/100 ml, however, adsorption amount per unit mass of ADRC decreased from 8.0 to 3.7 mg/g. This may be due to the decrease in total adsorption surface area available to MG resulting from overlapping or aggregation of adsorption sites [23].

3.4. Effect of initial MG concentration

The effect of initial concentration on the adsorptive removal of MG by ADRC is shown in Fig. 6. It can be observed that unit adsorption increased while the percentage adsorption decreased with increase in initial MG concentration. The MG ions around absorbent sites of adsorbent became much more with the increase of initial MG concentration. Hence, the adsorption process was carried out more sufficient resulting in the increase of unit adsorption.

3.5. Adsorption isotherms

Various isotherms [17] such as Freundlich, Langmuir, Dubnin–Radushkevih (D–R), Redlich–Peterson (R–P) and Temkin isotherm have been used to describe the equilibrium characteristics of adsorption in order to design the adsorption system and evaluate the applicability of sorption process. In this study, two most common isotherms, namely the Freundlich and Langmuir isotherm, were applied to analyze the adsorption equilibrium experimental data.

The Freundlich isotherm [34] is an empirical equation employed to describe heterogeneous systems. It based on the assumption of a heterogeneous surface with interaction between adsorbed molecules and a non-uniform distribution of adsorption heat over the surface. The Freundlich isotherm equation is expressed by the following equation:

$$q_e = K_F C_e^{1/n} \tag{3}$$

where q_e is the amount of dye adsorbed at equilibrium (mg/g), C_e the equilibrium dye concentration in solution (mg/l), K_F the Freundlich constant ((mg/g)(l/mg)$^{1/n}$) and $1/n$ is the heterogeneity factor which are related to the capacity and intensity of the adsorption, respectively. The linear form of Freundlich isotherm equation is

$$\ln q_e = \ln K_F + \frac{1}{n} \ln C_e \tag{4}$$

Therefore, the values of K_F and $1/n$ can be obtained from the slope and the intercept of the plot of $\ln q_e$ versus $\ln C_e$.

Langmuir isotherm [35] assumes that sorption occurs at specific homogenous sites within the adsorbent and the capacity of the adsorbent is finite. The equation of Langmuir is represented as follows:

$$q_e = \frac{K_L q_m C_e}{1 + K_L C_e} \tag{5}$$

where q_m is monolayer adsorption capacity (mg/g), K_L is Langmuir isotherm constant related to the affinity of the binding sites and energy of adsorption (l/mg). A well-known linear form of Langmuir equation is written as

$$\frac{C_e}{q_e} = \frac{C_e}{q_m} + \frac{1}{K_L q_m} \tag{6}$$

Therefore, the values of q_m and K_L can be calculated by plotting C_e/q_e versus C_e. The essential characteristics of a Langmuir isotherm can be expressed in terms of a dimensionless constant separation factor or equilibrium parameter, R_L [36], which is defined by

$$R_L = \frac{1}{1 + K_L C_0} \tag{7}$$

where C_0 is the initial dye concentration (mg/l) and K_L is Langmuir isotherm constant (l/mg). The R_L values indicate the type of the isotherm to be either unfavorable ($R_L > 1$), linear ($R_L = 1$), favorable ($0 < R_L < 1$) or irreversible ($R_L = 0$).

Fig. 7 shows the plots of $\ln q_e$ versus $\ln C_e$ and the plots of C_e/q_e versus C_e for the adsorption of MG onto ACRC at 293, 303 and 313 K according to the linear forms of Freundlich and Langmuir isotherm. The constants values calculated from the linear forms of the two isotherms are given in Table 1.

From Table 1, the values of $1/n$ were found to be less than 1 for all temperatures indicating that the adsorption was favorable

Table 1
Isotherm parameters obtained by using linear method for the adsorption of MG onto ADRC at different temperatures

	Temperature (K)		
	293	303	313
Freundlich			
K_F ((mg/g)(l/mg)$^{1/n}$)	3.93	4.64	5.45
$1/n$	0.196	0.170	0.156
R^2	0.8462	0.8340	0.9335
Langmuir			
q_m (mg/g)	8.49	8.69	9.35
K_L (l/mg)	0.35	0.58	0.97
R_L	0.028–0.088	0.017–0.054	0.010–0.033
R^2	0.9991	0.9997	0.9997

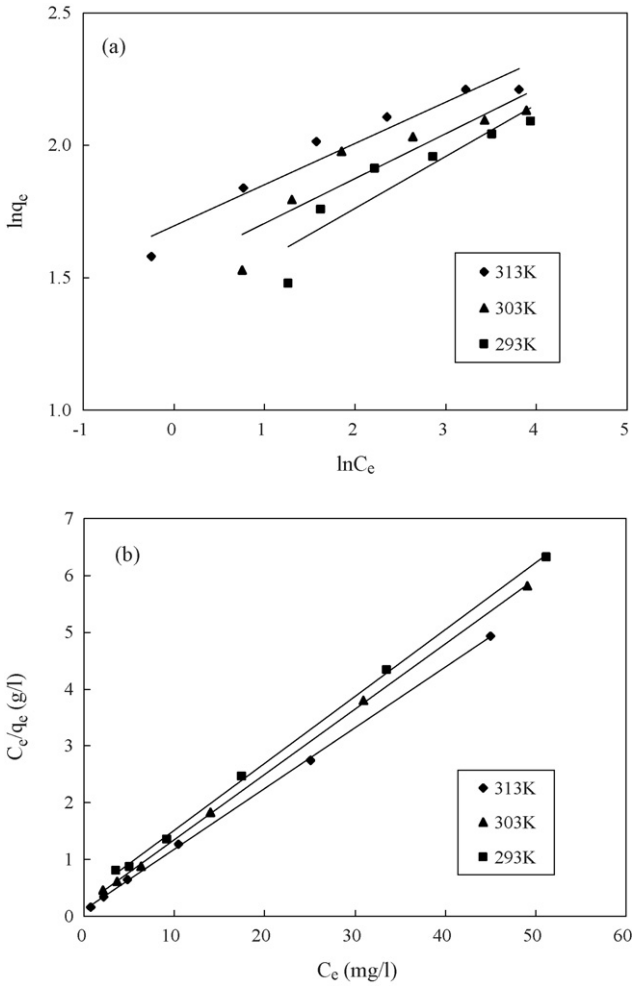

Fig. 7. Adsorption isotherms using linear method for MG onto ADRC at different temperatures: (a) Freundlich and (b) Langmuir isotherm (C_0 = 30, 40, 50, 60, 80 and 100 mg/l, ADRC dosage = 0.6 g/100 ml, pH 5, t = 180 min).

[37]. The R_L value in the range 0–1 also confirmed the favorable adsorptive uptake of dye process. Further from Table 1, it was observed that the values of linear correlation coefficient, R^2, were at a range between 0.8340 and 0.9335 for Freundlich isotherm, while for Langmuir isotherm were between 0.9991 and 0.9997, indicating that Langmuir isotherm better represented the experimental adsorption data at all solution temperatures. The fact that Langmuir isotherm fits the experimental data very well suggests the monolayer coverage of MG onto ADRC surface as well as the homogenous distribution of active sites on the ADRC surface, for the Langmuir isotherm assumes that the surface is homogenous. Further seen from Table 1, the values of q_m and K_F increased with the increase in temperature indicating that the adsorption process is endothermic in nature.

The adsorption capacities of MG onto some low-cost adsorbents are given in Table 2. From Table 2, the adsorption capacity of ADRC was found to be 8.69 mg/g and was comparable to those of some other adsorbents.

The non-linear method [38] was also used in this study to determine the best-fit isotherm. The experimental data and the predicted equilibrium curves using non-linear method for the two isotherms are shown in Fig. 8. The obtained isotherm parameters were listed in Table 3. In this paper, the non-linear chi-square test statistic, χ^2 [39], was examined to confirm the best-fit isotherm for the adsorption system. χ^2 is expressed by

$$\chi^2 = \sum \frac{(q_{e,exp} - q_{e,cal})^2}{q_{e,cal}} \quad (8)$$

where $q_{e,exp}$ and $q_{e,cal}$ are experimental and calculated q_e values, respectively. If data from model are similar to the experimental

Table 2
Comparison of adsorption capacities of MG onto low-cost adsorbents

Adsorbent	q_m (mg/g)	Reference
Bagasse fly ash	170.3	[30]
Waste apricot	116.3	[17]
Activated slag	74.2	[31]
Iron humate	19.2	[29]
Arundo donax root carbon	8.69	This study
Bentonite clay	7.72	[27]
Sugar cane dust	4.88	[5]
Activated charcoal	0.179	[26]

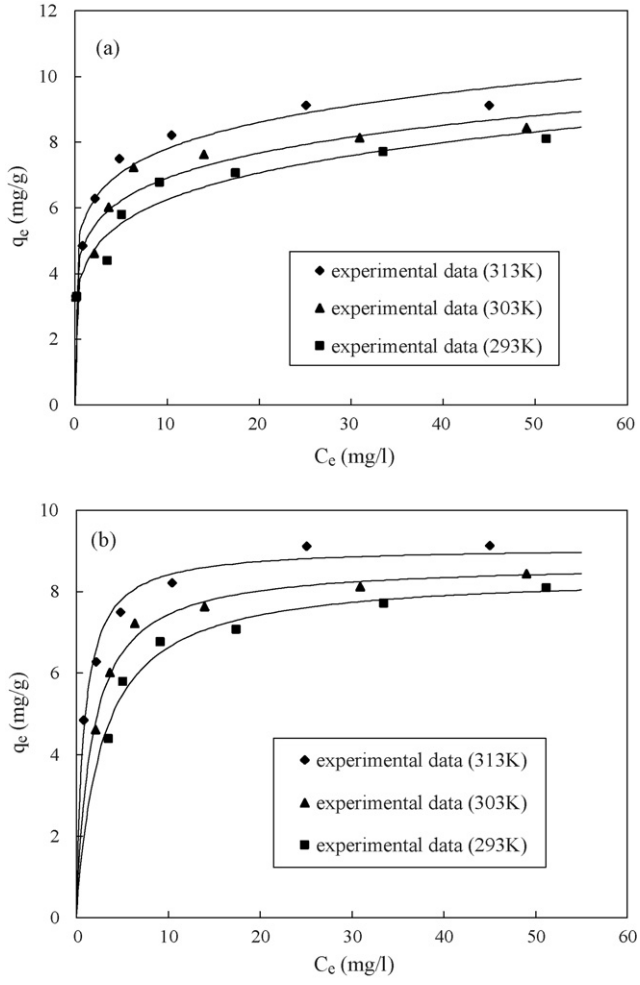

Fig. 8. Adsorption isotherms using non-linear method for MG onto ADRC at different temperatures: (a) Freundlich and (b) Langmuir isotherm (C_0 = 30, 40, 50, 60, 80 and 100 mg/l, ADRC dosage = 0.6 g/100 ml, pH 5, t = 180 min).

Table 3
Isotherm parameters obtained by using non-linear method for the adsorption of MG onto ADRC at different temperatures

	Temperature (K)		
	293	303	313
Freundlich			
K_F ((mg/g)(l/mg)$^{1/n}$)	4.15	4.88	5.63
$1/n$	0.178	0.151	0.142
r^2	0.8713	0.8467	0.9285
χ^2	0.211	0.262	0.145
Langmuir			
q_m (mg/g)	8.44	8.70	9.10
K_L (l/mg)	0.37	0.59	1.23
R_L	0.026–0.082	0.017–0.053	0.008–0.026
r^2	0.9593	0.9788	0.9634
χ^2	0.067	0.034	0.082

data, χ^2 will be a smaller number; if they are different, χ^2 will be a larger number. The non-linear correlation coefficient, r^2, and χ^2 were obtained and also shown in Table 3. Seen from Table 3, higher r^2 value and smaller χ^2 value of Langmuir isotherm compared to the r^2 value and χ^2 value of Freundlich isotherm confirmed that Langmuir isotherm was the better fit isotherm to represent the experimental data.

3.6. Thermodynamics study

Thermodynamic parameters including Gibbs free energy change (ΔG), enthalpy change (ΔH) and entropy change (ΔS) were calculated from the following equations [2,36]:

$$\Delta G = -RT \ln K \quad (9)$$

$$\Delta G = \Delta H - T\Delta S \quad (10)$$

where R is the gas constant, T is temperature in K and K is Langmuir constant (l/mol, obtained from slop and intercept of C_e/q_e versus C_e (mol/l) plot) at different temperatures. The values of ΔH and ΔS were determined from the slope and intercept of the plot of ΔG versus T. Thermodynamic parameters obtained are shown in Table 4.

From Table 4, the values of ΔG were found to be −28.61, −30.90 and −33.24 kJ/mol at 293, 303 and 313 K, respectively. The ΔG value is negative for all the temperatures, indicating that the adsorption is spontaneous process. The positive values of ΔH as shown in Table 4 indicate the endothermic nature of the process. The values of ΔS are positive, reflecting the affinity of the adsorbent material towards MG.

Table 4
Thermodynamic parameters for the adsorption of MG onto ADRC at different temperatures

Temperature (K)	ΔG (kJ/mol)	ΔH (kJ/mol)	ΔS (kJ/mol K)
293	−28.61	39.16	0.231
303	−30.90	39.16	0.231
313	−33.24	39.16	0.231

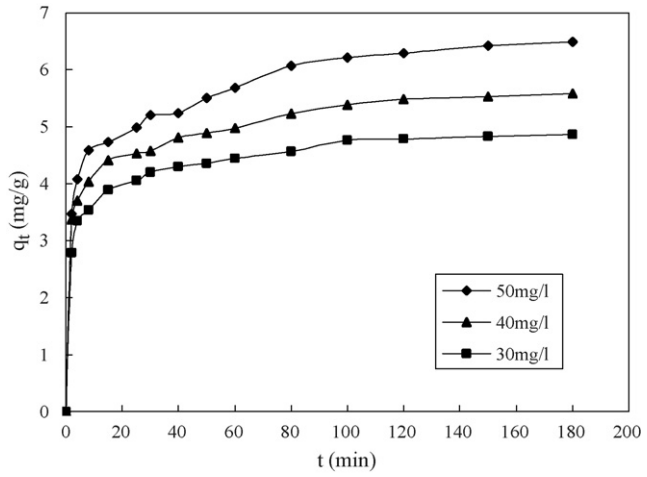

Fig. 9. Effect of contact time on the adsorption of MG by ADRC (C_0 = 30, 40 and 50 mg/l, ADRC dosage = 0.6 g/100 ml, pH 5, temperature = 30 ± 1 °C).

3.7. Effect of contact time

Fig. 9 shows the effect of contact time on the removal of MG by ADRC for different initial dye concentration. The adsorption was rapid in the initial 30 min and thereafter, the rate of adsorption decreased gradually. At some point in time, when the amount dye being adsorbed onto the adsorbent was equal to the amount dye being desorbed from the adsorbent, the adsorption process reached a dynamic equilibrium and the adsorption amount remained approximately a constant. It was observed from contact time curves that the equilibrium time was 180 min for all dye concentration. This is the reason why the optimum contact time was 180 min in above batch equilibrium experiments. The curves are single, smooth and continuous leading to saturation, also indicating the possible monolayer coverage of dye on the surface of the adsorbent [40].

3.8. Adsorption kinetics study

Three kinetic models were applied in this study to investigate the adsorption process of MG onto ADRC.

The pseudo-first-order Lagergren equation is given as [41]:

$$\log(q_e - q_t) = \log q_e - \frac{k_1}{2.303}t \quad (11)$$

where q_t and q_e are the amount adsorbed at time t and at equilibrium (mg/g) and k_1 is the pseudo-first-order rate constant for the adsorption process (min^{-1}).

The pseudo-second-order model can be represented in the following form [42]:

$$\frac{t}{q_t} = \frac{1}{k_2 q_e^2} + \frac{1}{q_e}t \quad (12)$$

where k_2 is the pseudo-second-order rate constant (g/mg min).

The plots of $\log(q_e - q_t)$ versus t and the plots of t/q_t versus t for different initial dye concentration are shown in Figs. 10 and 11. Kinetic constants calculated from slope and intercept of plots for the two models are given in Table 5. For pseudo-first-order model, the obtained R^2 values were relatively

Table 5
Parameters of pseudo-first-order and pseudo-second-order models for the adsorption of MG onto ADRC at different initial dye concentrations

C_0 (mg/l)	$q_{e,exp}$ (mg/g)	Pseudo-first-order			Pseudo-second-order		
		k_1 (min^{-1})	$q_{e,cal}$ (mg/g)	R^2	k_2 (g/mg min)	$q_{e,cal}$ (mg/g)	R^2
30	4.87	0.0265	1.96	0.9396	0.0456	4.94	0.9990
40	5.58	0.0260	2.43	0.9509	0.0340	5.67	0.9984
50	6.49	0.0249	3.18	0.9575	0.0233	6.63	0.9975

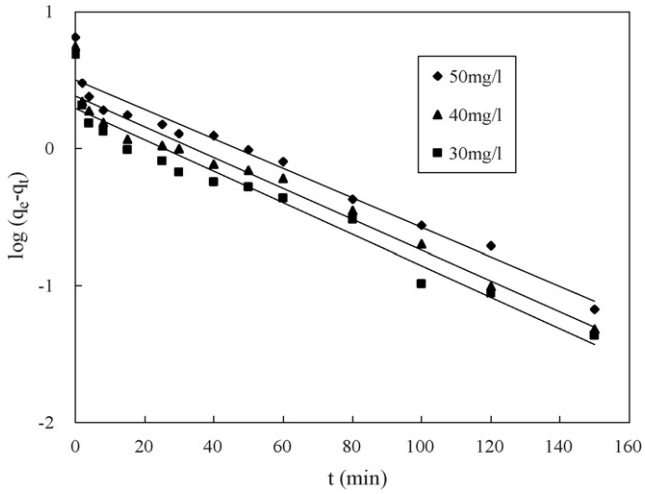

Fig. 10. Pseudo-first-order kinetics plots for MG onto ADRC at different initial dye concentrations (C_0 = 30, 40 and 50 mg/l, ADRC dosage = 0.6 g/100 ml, pH 5, temperature = 30 ± 1 °C).

small and the calculated q_e values ($q_{e,cal}$) were much lower than the experimental q_e values ($q_{e,exp}$). For pseudo-second-order model, the $q_{e,cal}$ values agreed very well with the $q_{e,exp}$ values and the R^2 values were also closer to 1. Therefore, the adsorption of MG onto ADRC can be well described by the pseudo-second-order model. Similar adsorption kinetic results of MG have also been obtained in literature [28,30]. From Fig. 11, the plots of t/q_t versus t were straight lines at the whole contact time for all

Table 6
Parameters of intraparticle diffusion model for the adsorption of MG onto ADRC at different initial dye concentrations

C_0 (mg/l)	k_{int} (mg/g min$^{1/2}$)	C (mg/l)	R^2
30	0.129	3.45	0.9801
40	0.173	3.66	0.9917
50	0.251	3.74	0.9819

the initial concentrations studied, suggesting that the adsorption process followed the pseudo-second-order kinetic model at the entire sorption time, which supported the assumption for the model that the adsorption is due to chemisorption [43]. Further seen from Table 5, the R^2 value increased from 0.9396 to 0.9575 for pseudo-first-order model while decreased from 0.9990 to 0.9975 for pseudo-second-order model with the increase in initial dye concentration from 30 to 50 mg/l, which supported the study results of Azizian [44] that with increasing initial concentration of the solute, the correlation of experimental data to pseudo-first-order kinetic model increases while that to the pseudo-second-order model decreases.

The intraparticle diffusion model was applied in this paper to determine if the rate-limiting step is intraparticle diffusion. The rate parameter for intraparticle diffusion is expressed as follows [45]:

$$q_t = k_{int} t^{1/2} + C \quad (13)$$

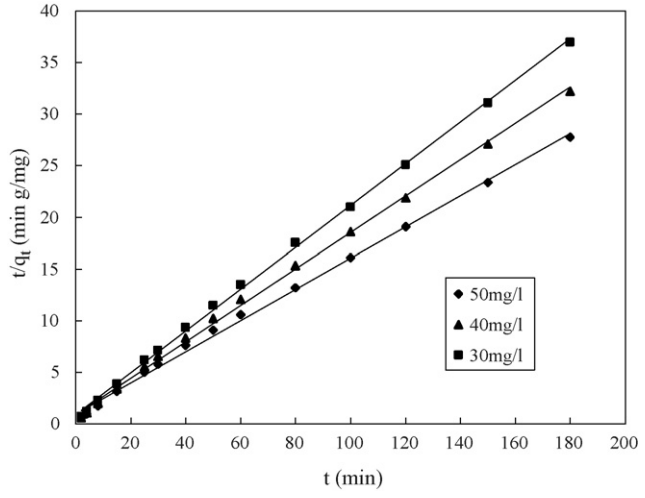

Fig. 11. Pseudo-second-order kinetics plots for MG onto ADRC at different initial dye concentrations (C_0 = 30, 40 and 50 mg/l, ADRC dosage = 0.6 g/100 ml, pH 5, temperature = 30 ± 1 °C).

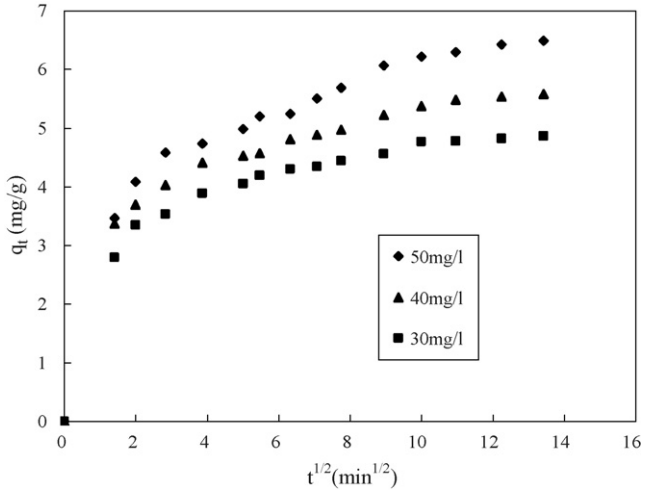

Fig. 12. Intraparticle diffusion plots for MG onto ADRC at different initial dye concentrations (C_0 = 30, 40 and 50 mg/l, ADRC dosage = 0.6 g/100 ml, pH 5, temperature = 30 ± 1 °C).

Table 7
Pseudo-first-order (k_1), pseudo-second-order (k_2) and intraparticle diffusion (k_{int}) rate constants for adsorption of MG on various adsorbents

Adsorbent	k_1 (min^{-1})	k_2 (g/mg min)	k_{int} (mg/g min$^{1/2}$)	Reference
Waste apricot	0.0697	2.86×10^{-3}	4.72	[18]
Sulphuric acid-treated sawdust	0.0534			[23]
Formaldehyde-treated sawdust	0.0332			[23]
Activated lignite carbon	0.0302	3.85×10^{-4}	9.5	[28]
Arundo donax root carbon	0.0260	0.0340	0.173	This study
Hen feather	0.0191			[25]
Bagasse fly ash	0.0168	0.394	6.7×10^{-3}	[30]
Modified peat	6.68×10^{-3}	2.52×10^{-3}	0.80	[32]
De-oiled soya	2.3×10^{-4}			[24]

where k_{int} is the intraparticle diffusion rate constant (mg/g min$^{1/2}$) and C is the intercept (mg/l). If the mechanism of adsorption process follows the intraparticle diffusion, the plot of q_t versus $t^{1/2}$ would be a straight line and the k_{int} and C can be calculated from the slop of the plot. C gives an idea about the thickness of the boundary layer, i.e., the larger the intercept the greater the boundary layer effect [28].

Fig. 12 shows the amount of MG adsorbed versus $t^{1/2}$ for different initial dye concentration. As seen from Fig. 12, the plots were multi-linear and there were three different portions, indicating the different stages in adsorption. The initial curved portion was attributed the bulk diffusion and the second linear portion was due to intraparticle diffusion [46]. The values of k_{int} and C were obtained from the second linear portion. The plateau following the second linear portion was the final equilibrium stage where intraparticle diffusion started to slow down due to the low dye concentration in the solution [47]. Table 6 shows the intraparticle diffusion parameters for the adsorption process. The values of R^2 for this model were at a range of 0.9801 and 0.9917, indicating that the adsorption followed the intraparticle diffusion model after 25 min. However, the lines did not pass through the origin. The deviation of the lines from the origin indicated that the intraparticle diffusion was not the only rate-limiting step [48] and boundary layer control may be involved in the process. The values of C were found from Table 6 increasing with the increase of initial concentration of MG, indicating increase in the thickness and the effect of boundary layer.

The rate constants (k_1, k_2 and k_{int}) of MG adsorption onto ADRC and other low-cost adsorbents are given in Table 7. Since the experimental conditions are not the same, a direct comparison of literature data obtained using different adsorbents is not possible. However, it was observed that the values of k_1, k_2 and k_{int} obtained in this study were comparable with those of some other adsorbents in Table 7.

4. Conclusion

ADRC was prepared from Arundo donax root by carbonization and the surface area was 158 m^2/g by N_2 isotherm. Adsorption of malachite green from aqueous solution onto ADRC has been studied. The adsorption was independent of operating variables including solution pH, carbon dose and initial MG concentration. In this study, the effective pH was 5–7 and the optimum adsorbent dose was found to be 0.6 g/100 ml. Langmuir isotherm gave a better fit to adsorption isotherms than Freundlich isotherm using linear and non-linear methods. Thermodynamic study showed that the adsorption process was spontaneous and endothermic since ΔG value was negative and ΔH value was positive. Adsorption reached equilibrium in 180 min contact time. The kinetic study confirmed that the adsorption followed pseudo-second-order model. The results of this study show that ADRC can be employed as a low-cost adsorbent in wastewater treatment for the removal of MG.

Acknowledgement

This work was supported by the National Natural Science Foundation of China.

References

[1] K.V. Kumar, S. Sivanesan, V. Ramamurthi, Adsorption of malachite green onto Pithophora sp., a fresh water algae: equilibrium and kinetic modelling, Process Biochem. 40 (2005) 2865–2872.
[2] V.K. Gupta, A. Mittal, L. Krishnan, V. Gajbe, Adsorption kinetics and column operations for the removal and recovery of malachite green from wastewater using bottom ash, Sep. Purif. Technol. 40 (2004) 87–96.
[3] S.J. Culp, L.R. Blankenship, D.F. Kusewitt, D.R. Doerge, L.T. Mulligan, F.A. Beland, Toxicity and metabolism of malachite green and leucomalachite green during short-term feeding to Fischer 344 rats and B6C3F1 mice, Chem. Biol. Interact. 122 (1999) 153–170.
[4] L. Papinutti, N. Mouso, F. Forchiassin, Removal and degradation of the fungicide dye malachite green from aqueous solution using the system wheat bran—Fomes sclerodermeus, Enzyme Microb. Technol. 39 (2006) 848–853.
[5] S.D. Khattri, M.K. Singh, Colour removal from dye wastewater using sugar cane dust as an adsorbent, Adsorp. Sci. Technol. 17 (1999) 269–282.
[6] G. Mckay, J.F. Porter, G.R. Prasad, The removal of dye colours from aqueous solutions by adsorption on low-cost materials, Water Air Soil Pollut. 114 (1999) 423–438.
[7] M.N. Khan, A. Sarwar, U. Zareen, Fahimuddin, Adsorption characteristics of crystal violet on beach sand from aqueous solution, Pak. J. Anal. Chem. 3 (2002) 8–12.
[8] V.K. Gupta, Suhas, I. Ali, V.K. Saini, Removal of rhodamine B, fast green and methylene blue from wastewater using red mud, an aluminum industry waste, Ind. Eng. Chem. Res. 43 (2004) 1740–1747.
[9] V.K. Gupta, A. Mittal, R. Jain, M. Mathur, S. Sikarwar, Adsorption of Safranin-T from wastewater using waste materials-activated carbon and activated rice husks, J. Colloid Interf. Sci. 303 (2006) 80–86.
[10] V.K. Gupta, A. Mittal, L. Kurup, J. Mittal, Adsorption of a hazardous dye, erythrosine, over hen feathers, J. Colloid Interf. Sci. 304 (2006) 52–57.

[11] V.K. Gupta, I. Ali, V.K. Saini, T.V. Gerven, B.V. Bruggen, C. Vandecasteele, Removal of dyes from wastewater using bottom ash, Ind. Eng. Chem. Res. 44 (2005) 3655–3664.
[12] A.K. Jain, V.K. Gupta, A. Bhatnagar, Suhas, Utilization of industrial waste products as adsorbents for the removal of dyes, J. Hazard. Mater. 101 (2003) 31–42.
[13] A.K. Jain, V.K. Gupta, A. Bhatnagar, S. Jain, Suhas, A comparative assessment of adsorbents prepared from industrial wastes for the removal of cationic dye, J. Indian Chem. Soc. 80 (2003) 267–270.
[14] V.K. Gupta, D. Mohan, S. Sharma, M. Sharma, Removal of basic dyes (rhodamine-B and methylene blue) from aqueous solutions using bagasse fly ash, Sep. Sci. Technol. 35 (2000) 2097–2113.
[15] V.K. Gupta, I. Ali, Suhas, D. Mohan, Equilibrium uptake and sorption dynamics for the removal of a basic dye (basic red) using low cost adsorbents, J. Colloid Interf. Sci. 265 (2003) 257–264.
[16] V.K. Gupta, I. Ali, Adsorbents for water treatment: Low cost alternatives to carbon, in: A. Hubbard (Ed.), Encyclopedia of Surface and Colloid Science, vol. 1, Marcel Dekker, New York, 2002, p. 136.
[17] C.A. Başar, Applicability of the various adsorption models of three dyes adsorption onto activated carbon prepared waste apricot, J. Hazard. Mater. 135 (2006) 232–241.
[18] Y. Önal, Kinetics of adsorption of dyes from aqueous solution using activated carbon prepared from waste apricot, J. Hazard. Mater. 137 (2006) 1719–1728.
[19] I.A. Rahman, B. Saad, S. Shaidan, E.S. Sya Rizal, Adsorption characteristics of malachite green on activated carbon derived from rice husks produced by chemical–thermal process, Biores. Technol. 96 (2005) 1578–1583.
[20] Y.P. Guo, H. Zhang, N.N. Tao, Y.H. Liu, J.R. Qi, Z.C. Wang, H.D. Xu, Adsorption of malachite green and iodine on rice husk-based porous carbon, Mater. Chem. Phys. 82 (2003) 107–115.
[21] Y.P. Guo, S.F. Yang, W.Y. Fu, J.R. Qi, R.Z. Li, Z.C. Wang, H.D. Xu, Adsorption of malachite green on micro- and mesoporous rice husk-based active carbon, Dyes Pigments 56 (2003) 219–229.
[22] V.K. Garg, R. Gupta, A.B. Yadav, R. Kumar, Dye removal from aqueous solution by adsorption on treated sawdust, Biores. Technol. 89 (2003) 121–124.
[23] V.K. Garg, R. Kumar, R. Gupta, Removal of malachite green dye from aqueous solution by adsorption using agro-industry waste: a case study of Prosopis cineraria, Dyes Pigments 62 (2004) 1–10.
[24] A. Mittal, L. Krishnan, V.K. Gupta, Removal and recovery of malachite green from wastewater using an agricultural waste material, de-oiled soya, Sep. Purif. Technol. 43 (2005) 125–133.
[25] A. Mittal, Adsorption kinetics of removal of a toxic dye, Malachite Green, from wastewater by using hen feathers, J. Hazard. Mater. 133 (2006) 196–202.
[26] M.J. Iqbal, M.N. Ashiq, Adsorption of dyes from aqueous solutions on activated charcoal, J. Hazard. Mater. 139 (2007) 57–66.
[27] S.S. Tahir, N. Rauf, Removal of a cationic dye from aqueous solutions by adsorption onto bentonite clay, Chemosphere 63 (2006) 1842–1848.
[28] Y. Önal, C. Akmil-Başar, D. Eren, Ç. Sarıcı-Özdemir, T. Depci, Adsorption kinetics of malachite green onto activated carbon prepared from TunÇbilek lignite, J. Hazard. Mater. 128 (2006) 150–157.
[29] P. Janoš, Sorption of basic dyes onto iron humate, Environ. Sci. Technol. 37 (2003) 5792–5798.
[30] I.D. Mall, V.C. Srivastava, N.K. Agarwal, I.M. Mishra, Adsorptive removal of malachite green dye from aqueous solution by bagasse fly ash and activated carbon-kinetic study and equilibrium isotherm analyses, Colloid Surf. A 264 (2005) 17–28.
[31] V.K. Gupta, S.K. Srivastava, D. Mohan, Equilibrium uptake, sorption dynamics, process optimization and column operations for the removal and recovery of malachite green from wastewater using activated carbon and activated slag, Ind. Eng. Chem. Res. 36 (1997) 2207–2218.
[32] Q. Sun, L. Yang, The adsorption of basic dyes from aqueous solution on modified peat-resin particle, Water Res. 37 (2003) 1535–1544.
[33] T. Vernersson, P.R. Bonelli, E.G. Cerrella, A.L. Cukierman, Arundo donax cane as a precursor for activated carbons preparation by phosphoric acid activation, Biores. Technol. 83 (2002) 95–104.
[34] H.M.F. Freundlich, Uber die adsorption in lasungen, Z. Phys. Chem. 57 (1906) 385–470.
[35] I. Langmuir, The constitution and fundamental properties of solids and liquids, J. Am. Chem. Soc. 38 (1916) 2221–2295.
[36] K.R. Hall, L.C. Eagleton, A. Acrivers, T. Vermenlem, Pore and solid diffusion kinetics in fixed adsorption constant pattern conditions, Ind. Eng. Chem. Res. 5 (1966) 212–223.
[37] S.D. Faust, O.M. Aly, Adsorption Processes for Water Treatment, Butterworths, 1987.
[38] K.V. Kumar, Comparative analysis of linear and non-linear method of estimating the sorption isotherm parameters for malachite green onto activated carbon, J. Hazard. Mater. 136 (2006) 197–202.
[39] Y.S. Ho, A.E. Ofomaja, Kinetics and thermodynamics of lead ion sorption on palm kernel fibre from aqueous solution, Process Biochem. 40 (2005) 3455–3461.
[40] P.K. Malik, Use of activated carbons prepared from sawdust and rice-husk for adsorption of acid dyes: a case study of Acid Yellow 36, Dyes Pigments 56 (2003) 239–249.
[41] S. Lagergren, B.K. Svenska, Zur theorie der sogenannten adsorption geloester stoffe, Veterskapsakad Handlingar 24 (1898) 1–6.
[42] Y.S. Ho, G. McKay, Sorption of dye from aqueous solution by peat, Chem. Eng. J. 70 (1998) 115–124.
[43] K.V. Kumar, V. Ramamurthi, S. Sivanesan, Modeling the mechanism involved during the sorption of methylene blue onto fly ash, J. Colloid Interf. Sci. 284 (2005) 14–21.
[44] S. Azizian, Kinetic model of sorption: a theoretical analysis, J. Colloid Interf. Sci. 276 (2004) 47–52.
[45] W.J. Weber Jr., J.C. Morris, Kinetics of adsorption on carbon from solution, J. Sanit. Eng. Div. Am. Soc. Civ. Eng. 89 (1963) 31–59.
[46] S.J. Allen, G. Mckay, K.Y.H. Khader, Intraparticle diffusion of a basic dye-during adsorption onto sphagnum peat, Environ. Pollut. 56 (1989) 39–50.
[47] F.C. Wu, R.L. Tseng, R.S. Juang, Comparisons of porous and adsorption properties of carbons activated by steam and KOH, J. Colloid Interf. Sci. 283 (2005) 49–56.
[48] V.J.P. Poots, G. McKay, J.J. Healy, Removal of basic dye from effluent using wood as an adsorbent, J. Water Pollut. Control Fed. 50 (1978) 926–939.